Safety Assessment of Gender-specific Human Electromagnetic Exposure with Aortic Valve Stents for EV-WPT

Tianhong Tan[1], Tao Jiang[1], Yangyun Wu[2], Yu Zhu[2], and Yaodan Chi[3]

[1]College of Information and Communication Engineering
Harbin Engineering University, Harbin 150001, China
tthjob@163.com, jiangtao@hrbeu.edu.cn

[2]College of Instrumentation and Electrical Engineering
Jilin University, Changchun 130000, China
wuyangyun@jlu.edu.cn, zhuyu@jlu.edu.cn

[3]Jilin Provincial Key Laboratory of Architectural Electricity and Comprehensive Energy Saving Jilin Jianzhu University, Changchun 130118, China
147670107@qq.com

Abstract **–** Electric vehicle wireless power transfer brings additional electromagnetic exposure (EME) risks to the human body, especially those with metal implants. This paper focuses on the safety assessment of human EME with aortic valve stents (AVS), and establishes electromagnetic simulation models for different genders of humans, AVS, and electric vehicle-wireless power transfer (EV-WPT) systems. The transmission power of the EV-WPT system is 11 kW. Considering the uncertainty of the EV-WPT system and AVS in practical use, an efficient deep neural network method is proposed to evaluate the EME safety to different genders of humans. Using the standard limits of the International Committee on Non-Ionizing Radiation Protection (ICNIRP) as the judgment standard, comparing human EME under static conditions, it is demonstrated that AVS can change the distribution of induced electric fields in the human body and increase the risk of human EME. Moreover, the probability of male human EME exceeding the standard limits is 22.78% higher than that of female human.

Index Terms **–** Aortic valve stents (AVS), deep neural network, electric vehicle (EV), electromagnetic exposure safety, human model, wireless power transfer (WPT).

I. INTRODUCTION

Electric vehicles (EVs) are the core of future automotive technology development. Compared to plug-in charging, wireless power transfer (WPT) systems can save urban land space. Furthermore, the charging process is safe and reliable, enabling seamless charging [1]. More importantly, the electric vehicle-wireless power transfer (EV-WPT) system is a key link in improving intelligent driving. Therefore, the WPT system will be the development trend of future EV charging technology [2]. Due to the transmission of energy through open space [3], the EV-WPT system generates a large amount of leakage magnetic field, which inevitably exposes the nearby human body to the electromagnetic environment of the EV-WPT system. The safety of human electromagnetic exposure (EME) in the EV-WPT system has always been a focus of attention. In order to ensure the charging efficiency of EV and avoid range anxiety [4], the charging power of EV-WPT systems is usually as high as several thousand watts or even ten thousand watts, which significantly increases the risk of human EME. Therefore, evaluating the safety issues of human EME around EV-WPT systems is of great significance [5].

In order to ensure the safe use of high-power EV-WPT systems, many international organizations have developed relevant standards for the leakage magnetic field of WPT systems [6–8]. For example, the International Committee on Non-Ionizing Radiation Protection (ICNIRP) has developed different standards based on the different operating frequencies of WPT systems. When the operating frequency of WPT systems is below 100 kHz, the safety of human EME is mainly based on non-thermal effects, so the standard of concern is the induced electric field intensity (induced-E). When the working frequency of the WPT system is higher than 100 kHz, the EME safety of the human body is mainly based on thermal effects, and the specific absorption rate (SAR) of the human body is the standard of concern. With the current working frequency of EV-WPT systems typically being 85 kHz, this paper adopts induced-E as the analysis object of human EME in EV-WPT systems. The American Society of Automotive Engineers divides the

Submitted On: July 10, 2024
Accepted On: October 4, 2024

https://doi.org/10.13052/2024.ACES.J.390810

EV-WPT system into multiple levels based on transmission power [9], including WPT1 corresponding to 3.7 kw, WPT2 corresponding to 7.7 kw, and WPT3 corresponding to 11.1 kw. Considering the pursuit of charging speed for EVs, the 11.1 kw WPT system has most prominent research value.

For the human body exposed to the leakage magnetic field of the EV-WPT system, key organs in the human body are most worthy of attention. The heart is one of the most important organs in the human body, and there are a large number of cardiovascular disease patients in the world. Among them, aortic valve stenosis often leads to coronary artery disease, causing myocardial infarction and resulting in patient death. To treat this disease, a mechanical (metal made) aortic valve stent (AVS) is usually implanted into a narrowed valve in the patient's body to achieve normal blood delivery function of the heart [10, 11]. When the human body implanted with AVS is exposed to the leakage magnetic field of the EV-WPT system, the metal stent may change the distribution of electromagnetic energy, where the tip and edge of the stent are more likely to cause induced-E in the human body to exceed the recommended standard limit, leading to harm to the human body. In the practical application of the EV-WPT system, there is a lot of uncertainty in the positional relationship between the human body and the EV-WPT system, and there is usually misalignment between the transmitting and receiving coils of the WPT system. At the same time, there is also uncertainty in the relevant parameters of the WPT system during the production and manufacturing process. The above uncertainties will propagate to the leakage magnetic field of the EV-WPT system, ultimately affecting the EME safety of the human body. Therefore, it is of great significance to comprehensively evaluate the EME safety of human bodies with AVS in the leakage magnetic field of the EV-WPT system, taking into full consideration the uncertainties.

The main contributions of this paper are as follows:

1. Considering the human body of different genders, this paper evaluates the EME safety of males and females in the leakage magnetic field of the EV-WPT system;
2. This paper proposes a more efficient deep neural network method to analyze the uncertainty quantification (UQ) problem of human EME safety;
3. This paper analyzes the quantification of uncertainty in the safety of human EME with AVS, and takes into account the uncertainty of implants. It intuitively demonstrates the EME risk of the human body with metal medical implants in the leakage magnetic field of the EV-WPT system.

The main structure of this paper is as follows. Section II introduces the current research status of human EME safety assessment in the EV-WPT system. In section III, the human body model, AVS model, EV model, WPT system model, and human EME scenario are discussed. In section IV, the UQ method of our proposed deep neural network is introduced. Section V presents and analyzes the numerical experimental results of quantifying the safety uncertainty of human EME with AVS, and provides a detailed discussion. Section VI summarizes our research content and introduces our next research work.

II. RELATED WORK

EV-WPT technology is one of the most promising technologies, but it is accompanied by concerns about the electromagnetic safety of EV-WPT systems. Due to ethical issues in medicine and limitations in current technological levels [12], it is very difficult to measure the electromagnetic field inside the human body. Therefore, current research mainly focuses on numerical simulation, and analyzes the safety issues of human exposure to the electromagnetic environment of the EV-WPT system by establishing corresponding models in simulation software [13]. El-Shahat et al. [14] established an electromagnetic simulation model between the EV-WPT system and the human body, measured human EME at different distances, and analyzed the safe distance between the human body and the EV-WPT system. Chakarothai et al. [15] compared the numerical simulation results of human exposure in the electromagnetic environment of the EV-WPT system with experimental measurements, and derived the EME of the human body at different distances. Choi et al. [16] evaluated the electromagnetic safety issues of an EV-WPT system with a power of 20 kw, analyzed the EME values of the surrounding human body in the presence of offset between the transmitting and receiving coils, and compared them with the standard limits. The results showed that the basic limits of human fat and muscle were exceeded. Christ et al. [17] evaluated the exposure of the human body near the WPT system and analyzed it using four human models. They found that the intensity of human EME is closely related to the coil design and distance of the WPT system. Park [18] designed and established an electromagnetic simulation model for the EV-WPT system, and analyzed the human EME dose of the WPT system under different exposure scenarios, including shielded, unshielded, coil aligned, and coil misaligned conditions. By comparing with standard limits, the maximum transmission power and minimum safe distance of the EV-WPT system were proposed. Wang et al. [19] evaluated the human EME safety of an EV-WPT system with a power of 10 kw. They analyzed three human models and

three exposure fields and, based on the results, proposed recommendations for the maximum power of the EV-WPT system and three protective measures for human EME safety.

In addition to the aforementioned studies, researchers have also noticed the risks of metal implants in the human body exposed to electromagnetic fields and conducted research. Shah et al. [20] established EV-WPT system models with different power levels and analyzed the intensity of induced-E in human bodies with multiple metal implants. In the simulation results, it was observed that the induced-E at the tibial intramedullary nail exceeded the standard limit of ICNIRP. Meanwhile, Shah et al. [21] evaluated the safety of human EME around EV-WPT systems operating at radio frequencies. The analysis results showed that when the human body with implants is located near the EV-WPT system, the SAR in the human body will exceed the standard limit.

In the above studies, many researchers have focused on the impact of misalignment between the transmitting and receiving coils of the EV-WPT system on human EME safety. This is actually an undeniable uncertainty in the application process of the EV-WPT system, and metal implants also have uncertainty, which can significantly affect the distribution of electromagnetic fields in the human body. However, the existing main research only considers these situations as fixed exposure scenarios, especially in the EV-WPT system where there is more than one type of uncertainty, resulting in incomplete evaluation results of human EME safety. Currently, few studies have considered the impact of uncertainty on the safety of human EME. Wang et al. [22] considered the uncertainty of geometric parameters and human position in the EV-WPT system, and quantitatively analyzed the uncertainty of human EME safety based on spectral methods. However, they did not take into account the potential impact of metal implants on the evaluation results. In [23], the influence of metal implants was considered, but the research subjects were males only. The uncertainty quantification method used was probability driven, and the computational cost would increase with the increase of variable dimensionality, leading to the problem of ”curse of dimensionality”. Therefore, in response to the shortcomings in the above research, this article takes male and female models with heart AVSs around the EV-WPT system as the research objects, considers uncertain exposure scenarios in practical applications, proposes an efficient deep neural network method to quantify the uncertainty of human EME safety, analyzes the statistical probability of risks exceeding standard limits, and intuitively evaluates human EME safety.

III. MATH

A. EV and WPT system

Firstly, the EV-WPT device model established in this article consists of an EV and a magnetic coupled WPT device. The EV model in this paper is constructed based on a pure electric sports car model with excellent power performance. As shown in Fig. 1, its spatial geometric dimension is $4520\times2050\times1260$ mm. Considering that real sports cars need to balance lightweight, high rigidity, and stability, the body and wheels of this article are made of aluminum alloy material, the front and rear windshields and windows are made of polycarbonate material, and the tires are made of rubber material. The size and material of the above EV model fully meet the requirements of this study.

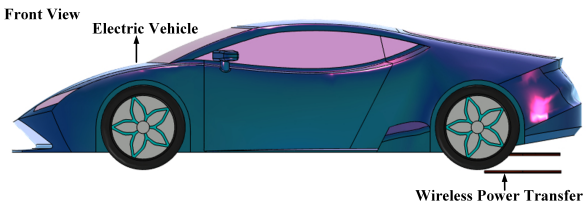

Fig. 1. EV model.

The working principle of the WPT system is shown in Fig. 2 . The power grid inputs AC power, which is converted into DC power through a rectifier circuit at the transmitting end. The DC power is then converted into higher frequency AC power through a high-frequency inverter circuit. The output power frequency of the inverter circuit is the resonant frequency of the transmitting resonant circuit. At this time, the transmitting circuit works in a resonant state under the action of the compensating circuit at the transmitting end, presenting pure resistance. According to Faraday’s law of electromagnetic induction, the transmitting coil excites a high-frequency electromagnetic field with a resonant frequency in space, which is induced and received by the receiving end coil. At this time, under the action of the receiving end compensation circuit, the receiving end circuit works in a resonant state and also presents pure resistance. The receiving end rectification circuit and DC-DC circuit convert the high-frequency power supply into the DC power required by the load, achieving wireless energy transmission. The magnetic coupling WPT device in this article equivalently converts the transmitting and receiving circuits. The transmitting and receiving devices are considered as shown in Fig. 3 . The transmitting device consists of a transmitting metal electromagnetic shielding layer and a transmitting coil (Tx), while the receiving device consists of a receiving metal

electromagnetic shielding layer and a receiving coil (Rx). The geometric dimensions of the transmitting and receiving electromagnetic shielding layers are the same, both 620×620×8 mm (A×A). The material selection is ferrite material, which is commonly used for electromagnetic shielding. The wire diameters of Tx and Rx are 2.5×10^{-6} and 1.8×10^{-6} mm^2, with 15 and 20 turns, respectively.

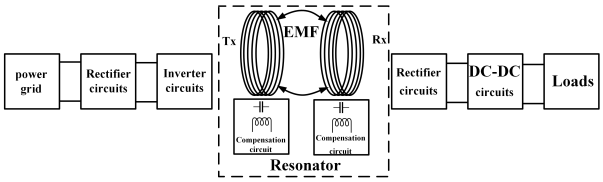

Fig. 2. Working principle of WPT system.

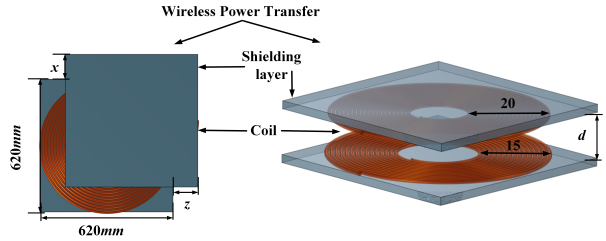

Fig. 3. WPT geometric model.

In order to improve the transmission performance of the magnetic coupled WPT device, an LCC-LCC topology compensation network structure is adopted in this article, as shown in Fig. 4 . Among them, I_0 is the equivalent current source at the transmitting end of the linear WPT circuit model, U_1 is the terminal voltage of the equivalent current source at the transmitting end, and L_{s1} and L_1 are the resonant inductance at the transmitting end and the self-inductance of Tx, respectively. The isolation capacitance and resonant capacitance at the corresponding transmitting end are C_{p1} and C_{s1}, respectively. R_{s1} and R_1 are the internal resistance of L_{s1} and Tx, respectively. M is the mutual inductance between the transmitter and receiver. Similarly, L_{s2} and L_2 are the resonant inductance at the receiving end and the self-inductance of Rx, respectively. The isolation capacitance and resonant capacitance at the receiving end are C_{p2} and C_{s2}, respectively. R_{s2} and R_2 are the internal resistances of L_{s2} and Tx, respectively. R_L is the resistance of the load carried by the WPT device, and U_2 is the terminal voltage of the load at the receiving end. When the LCC-LCC topology compensation circuit operates in a resonant state, the following resonant conditions apply.

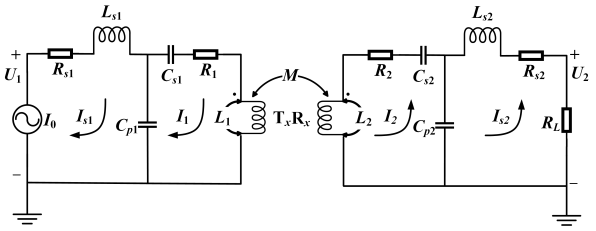

Fig. 4. LCC-LCC topology compensation circuit.

Resonance conditions at the transmitting end:

$$\omega L_1 - \frac{1}{\omega C_{s1}} = \frac{1}{\omega C_{p1}} = \omega L_{s1}. \tag{1}$$

Resonance conditions at the receiving end:

$$\omega L_2 - \frac{1}{\omega C_{s2}} = \frac{1}{\omega C_{p2}} = \omega L_{s2}. \tag{2}$$

When the magnetic coupled WPT device operates at a resonant frequency of 85 kHz and there are no dislocations at the transmitting and receiving ends, this paper considers its transmission power to be 11 kW.

B. Male and female human models

This paper considers the inconsistency of body fat and muscle content between males and females. In order to obtain the differences in EME between males and females, human models of males and females were established using Comsol finite element numerical simulation software, as shown in Fig. 5 . Among them, the male

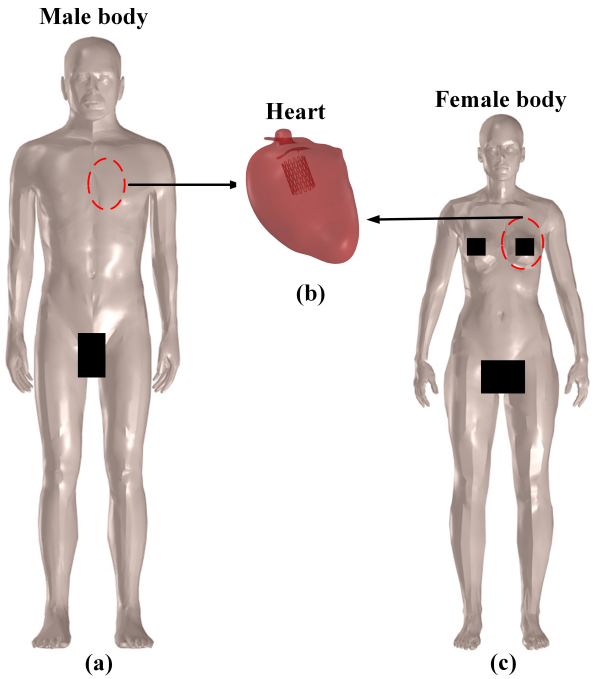

Fig. 5. (a) Male human model, (b) heart with AVS, and (c) female human model.

human model has a height of 1.80 m and a weight of 77 kg, while the female model has a height of 1.68 m and a weight of 55 kg.

The resonant transmission frequency of the EV-WPT device in this article is 85 kHz, the conductivity of male human tissue is considered to be 0.27 s/m, and the relative permittivity is 5500. The electrical conductivity of female human tissue is considered to be 0.23 s/m, with a relative permittivity of 5300. The conductivity of cardiac tissue is considered to be 0.21 s/m, with a relative permittivity of 11137 [20, 22]. According to ICNIRP 2010, when the electromagnetic field radiation frequency is less than 100 kHz, the induced-E inside the human body is the main measurement target. Therefore, this article uses induced-E as the indicator for calculating human EME. In addition, according to the recommendations of ICNIRP, when calculating the induced-E of the human body, the mesh division of the human body model should be within $2\times2\times2$ mm^3, the mesh division for male and female body models in this article adopts $0.9\times0.9\times0.9$ mm^3, which meets the recommendations of ICNIRP.

C. AVS

This paper evaluates the electromagnetic safety issues of the leakage electromagnetic field generated during the operation of the EV-WPT device on human bodies of different genders containing metal medical implants. The heart is the engine of the human body, which circulates blood to various parts of the body through contraction and relaxation. However, among cardiovascular diseases, the incidence rate and mortality rate of aortic valve disease is the second highest in the world [24]. Every year, nearly 30000 patients worldwide receive AVS replacement [25]. AVS is used to replace diseased valves to achieve the recovery of cardiac pumping function. Figures 6 (a-c) show the front and top views of the AVS customary in this paper. The length of the AVS is 26.7 mm and the diameter is 20 mm. The AVS is composed of 45 diamond shaped structures,

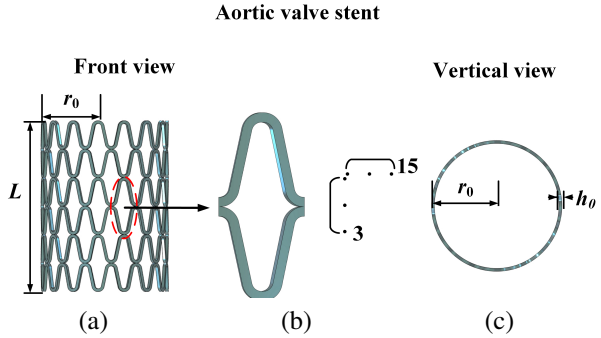

Fig. 6. Implant model.

each with a thickness of 0.45 mm and an edge width of 0.45 mm. Considering the biological safety, compatibility, and high strength of titanium alloy, nickel titanium alloy is chosen as the material for the AVS, with the following electromagnetic parameters: conductivity of 2.38×10^6 S/m, with a relative dielectric constant of 1. The sharp edge of metal implants can affect the distribution of electromagnetic fields and have the potential to absorb electromagnetic energy. Considering the high precision and multi tip of the AVS in this article, its mesh is divided into a finer resolution of $0.15\times0.15\times0.15$ mm^3.

D. Electromagnetic field analysis and calculation

To analyze the alternating electromagnetic field generated by magnetic coupled WPT using near-field theory, the electromagnetic field generated by resonators can be divided into radiated electromagnetic field and induced electromagnetic field by their properties. There is a 90° phase angle between the magnetic field and the electric field of the induced electromagnetic field. The electromagnetic energy of the induced electromagnetic field exchanges with each other during electromagnetic oscillations, flowing back and forth between the surrounding space and the resonator, without external radiation. In contrast, the radiated electromagnetic field is detached from the electromagnetic coupling resonator and radiated externally. According to the distance from the radiation source, the induced electromagnetic field and the radiated electromagnetic field are divided into near-field and far-field. The field intensity in the far-field decays with increasing distance. When the distance from the resonator is multiple wavelengths, only the electromagnetic radiation field needs to be considered. When the distance from the resonator is within the $\lambda/2\pi$ (λ is the wavelength), only the induced electromagnetic field needs to be considered. When working in the near-field, there is only electromagnetic field flow around and between the resonator, and there is no emission in the distance. Only by working in the near-field space can efficient energy transfer be achieved between the fields and circuits of the electromagnetic resonant WPT device.

When analyzing the numerical calculation of the electromagnetic field generated by magnetic coupled WPT, the magnetic quasi-static (MQS) method is used to solve the electromagnetic field value considering that the wavelength of the electromagnetic wave in space is larger than the geometric shape of the target to be solved. The criteria for using the MQS method are as follows [26]:

$$|\alpha^2|d^2 \ll 1, \tag{3}$$

$$\alpha^2 = \omega(\omega\varepsilon_r + j\sigma)\mu_0. \tag{4}$$

Among them, α is the wavenumber and d is the diameter of the calculation area. In the absence of

damage, the relationship between α and wavelength λ is $\alpha=2\pi/\lambda$, ω is the angular frequency of the electromagnetic field, the dielectric constant and conductivity of ε_r and σ human tissues, and μ_0 is the value of vacuum permeability $4\pi \times 10^{-7}$ (H/m).

In this paper, the transmission frequency of the magnetic coupled EV-WPT device is 85 kHz, and the electromagnetic wavelength generated in the near-field is about tens of meters [26]. When analyzing the electromagnetic field values at this frequency, the size of the target is much smaller than the wavelength of the electromagnetic wave, and the MQS method can be used to solve it.

E. Exposure scenario

The WPT system transmits energy through an open, loosely coupled structure, thus posing a higher risk when the human body is exposed without obstruction. Considering the practical situation of the EV-WPT system in daily use, the vehicle chassis is usually composed of metal, which has a certain shielding effect. Therefore, this paper mainly considers the situation where the human body is located outside the vehicle, and takes the exposure scene when the human body is located at the rear of the vehicle as the research object, as shown in Fig. 7.

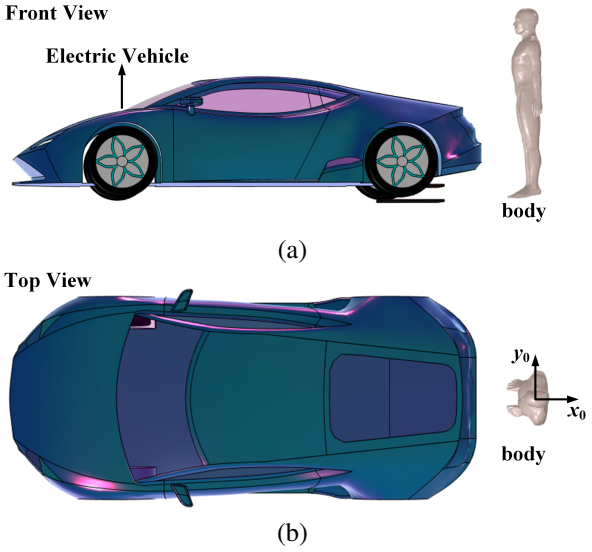

Fig. 7. Electromagnetic exposure scenarios.

IV. UNCERTAINTY QUANTIFICATION METHOD BASED ON DEEP NEURAL NETWORKS

In recent years, UQ based on machine learning theory has been vigorously promoted as an emerging technology, among which classic methods include Bayesian neural network prediction, Markov chain, Monte Carlo, approximate variational inference, etc. These methods have been successfully applied in multiple fields such as drone driving, moving object detection, and image processing, effectively achieving multiple functions such as probability statistical moment estimation and risk assessment. In the actual scenario of wireless energy transmission in EVs, considering the influence of uncertain factors such as misalignment of coupling coil groups caused by improper driver operation and errors in the manufacturing process of system components, the human EME indicators located around the wireless charging device also have strong uncertainties. Therefore, it is urgent to carry out human EME safety assessment and analysis.

This paper focuses on the induced-E of the heart with an AVS in the human body as the research objective. Deep neural networks are used to quantify the uncertainty of the induced-E of the human body under the exposure environment of the EV-WPT system, and the probability density distribution of the induced electric field strength value is obtained. The neural network itself consists of many hidden layers. Assuming that the input of a single node in the hidden layer is x and the output is y, the relationship between y and x can be expressed as:

$$y = \sigma(w \cdot x + b), \tag{5}$$

where $\sigma(\cdot)$ represents a nonlinear transfer function, w is a linear mapping, and b is the bias term. The RELU function is selected as the $\sigma(\cdot)$ function for the nodes in the hidden layer. Before starting to train the network model, the values of w and b are randomly assigned. During the model training process, the values of w and b are continuously updated until the error between the output result and the training label is approximately zero. The specific evaluation index function can be expressed as:

$$E^{w,b}(x,y) = \frac{1}{2N}\sum_{i=1}^{N} \|y_i - y^*\|^2, \tag{6}$$

where N represents the number of training samples, y_i represents the network output value, and y^* represents the training label. When $E^{w,b}(x,y)$ approaches infinity, it indicates that the current network training effect is relatively ideal. Based on the actual situation, random variables that may affect the induced-E of the human body are selected in the article, including the offset parameters of the transmitting and receiving coils, resonance compensation circuit parameters, metal implant parameters, and position parameters between the human body and the car. Trace data is collected from the distribution range of these variables as training set samples, and the induced-E corresponding to each group of samples are used as training labels, based on this, to train the deep neural network model.

The deep neural network constructed in the paper consists of multiple sub-models and adopts ensemble learning to effectively improve the computational accu-

racy and efficiency of the output end. Among them, each sub-model of the network is composed of three modules. The input of the first module is z_0, x_0, d_0, r_0, h_0. The input of the second module is th, c_1, c_2, cf_1, cf_2, lf_1 and the output of the first module. The input of the third module is lf_2, z_1, x_1 and the output of the second module. Finally, the predicted value of the human induced-E is obtained at the output end. The first part of the module consists of six fully connected layers and one batch normalization layer. The number of nodes in the first to last six fully connected layers is set to 5, 64, 32, 32, 16, and 1, respectively. The input feature number of the batch normalization layer is 32. Introducing a batch normalization layer can to some extent prevent overfitting in network training and strengthen the model's generalization ability. The specific normalization mathematical model can be expressed as:

$$y = \gamma \cdot \frac{x_i - E(x)}{\sqrt{var(x) + \varepsilon}} + \beta, \tag{7}$$

$$E(x) = \frac{1}{n}\sum_{i=1}^{n} x_i, \tag{8}$$

$$var(x) = \frac{1}{n}\sum_{i=1}^{n} (x_i - E(x))^2, \tag{9}$$

where γ and β are both parameter vectors, with default values of 0 and 1, respectively. ε is used to ensure numerical stability, with default values of 10^{-5}. The second part of the module consists of four fully connected layers, with the number of neuron nodes set to 7, 64, 32, and 1 in each layer from front to back. The third part of the module consists of five fully connected layers and a dropout layer. The number of nodes in the first to last five fully connected layers is 4, 64, 32, 16, and 1, respectively. The dropout function is similar to a batch normalization layer. By using the dropout module, some neural nodes can be randomly discarded, reducing the number of intermediate features and preventing the network model from being too close to the training set samples. Similarly, the overfitting effect can also be weakened to a certain extent. Figure 8 shows a comparison diagram of the dropout module applied before and after the network layer.

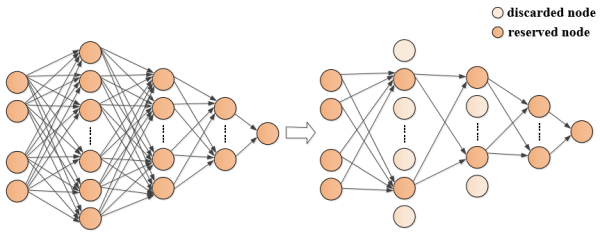

Fig. 8. Comparison of network layer structures before and after applying dropout.

After combining with the dropout module, the calculation formula for neuron nodes is updated to:

$$y_i^{l+1} = f(w_i^{l+1} \cdot r^l y^l + b_i^{l+1}), \tag{10}$$

$$r^l \sim Bernoulli(p), \tag{11}$$

where r^l represents a random number that follows a Bernoulli distribution and p represents the corresponding probability. Generally, the ideal value of p is 0.5. On the basis of the neural network model mentioned above, the paper adopts six model ensemble learning methods to merge the output of each sub-model to obtain more accurate prediction results.

Basic parameters such as the hidden layer structure and the number of training/testing samples for each sub-model are the same, with only differences in the number of training iterations and learning rate. Among them, the iteration numbers of the first three sub-models are set to 100, 200, and 400, respectively, and the learning rate is uniformly set to 10^{-3}. The iteration numbers of the last three sub-models are set to 600, 800, and 1000, respectively, and the learning rate is uniformly set to 2×10^{-3}. Figure 9 shows the basic structural framework of the integrated network model.

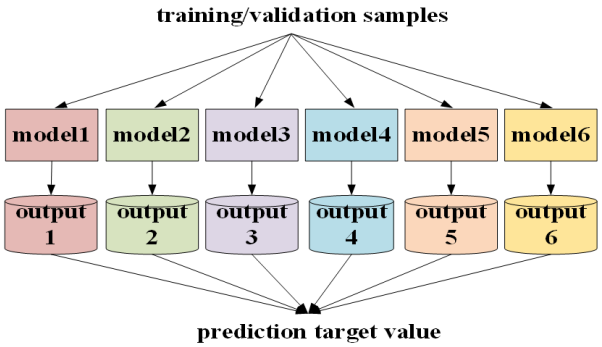

Fig. 9. Integrated prediction framework for multiple network models.

After the model training is completed, validation samples are collected from the distribution range of various related random variables as input, and the probability density distribution of human induced-E is finally obtained at the output end of the model, achieving quantitative safety assessment of human EME uncertainty in the wireless energy transmission environment of EVs. The pseudocode of the algorithm used in this paper is as follows:

V. SIMULATION RESULTS

A. Comparison of male and female body exposure under static conditions

The electromagnetic environment of the EV-WPT system under normal operation is shown in Fig. 10 . Based on the human EME scenario set in section III,

The uncertainty quantification based on deep neural network model

1.**While** the training iteration of model is below the maximum iterations
2. **For** the learning stage of first part of network module
3. update the weight threshold of first part of network module
4. **end for**
5. **For** the learning stage of second part of network module
6. update the weight threshold of second part of network module
7. **end for**
8. **For** the learning stage of third part of network module
9. update the weight threshold of third part of network module
10. **end for**
11. Get the output value
12. If the error of output value and training target meets the requirement, then complete the model training
13.**end while**
14.Obtain the probability density of heart's induced-*E* based on single neural network model
15.Calculate the probability density of heart's induced-*E* based on ensemble output of six models

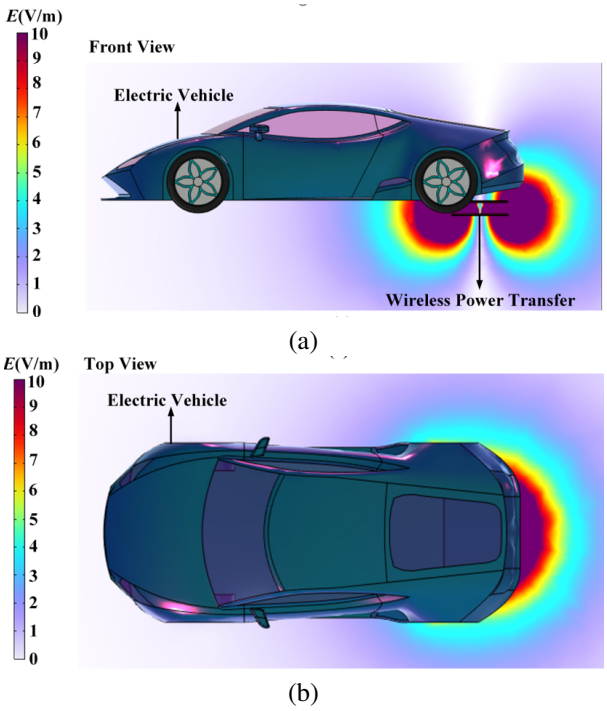

Fig. 10. EV-WPT system electromagnetic environment.

evaluate the safety issues of human EME using the EV-WPT system, male and female human body, and implant models established in this paper. Without considering uncertainty, that is, there is no offset between the transmitting and receiving coils of the WPT system, the resonance compensation circuit parameters are consistent with the design values, and the distance between the human body and the car is 0.2 m. Compare the EME of males and females without and with AVS, as shown in Figs. 11 and 12.

Observe the EME of the human body in Figs. 11 and 12, and compare the maximum value and location of the induced-*E* in different genders at this time, as shown in Table 1 . In the current exposure scenario, the induced-*E* in the male and female human bodies is basically the same and has not exceeded the standard limit of ICNIRP. Figures 11 and 12 illustrate the EME of male and female human bodies without considering the uncertainty variables listed in Table 2 . In this case, there is no significant difference in the leakage magnetic field distribution of the WPT system between males and females, indicating

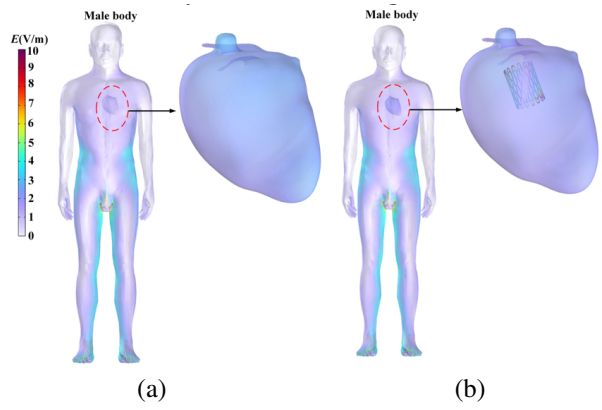

Fig. 11. Comparison of induced-*E* in male human body.

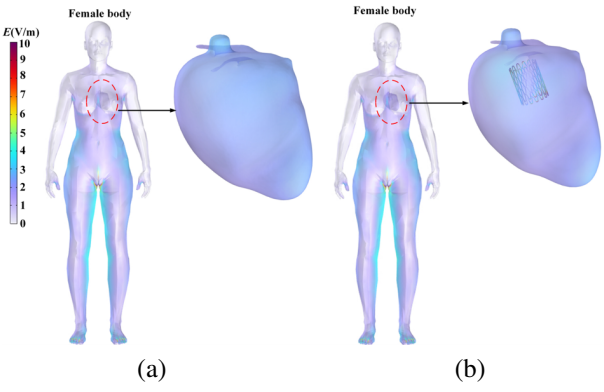

Fig. 12. Comparison of induced-*E* in female human body.

Table 1: The maximum value and location of induced-E in the human body

Gender	AVS	Induced-E_{max} (V/m)	Position
Male	Yes	4.765	Near AVS
	No	2.563	Human feet
Female	Yes	4.076	Near AVS
	No	2.324	Human feet

Table 2: The uncertainty of variables

Variables	Unit	Distribution Parameters
x	m	U [-0.075, 0.075]
z	m	U [-0.075, 0.075]
d	m	U [-0.05, 0.05]
r_0	mm	N [10, 3.33]
h_0	mm	N [0.45, 0.15]
th	mm	N [0.45, 0.15]
C_{s1}	f	N [7.98, 0.13] *10^{-9}
C_{s2}	f	N [11.94, 0.2] *10^{-9}
C_{p1}	f	N [32.64, 0.54] *10^{-9}
C_{p2}	f	N [21.52, 0.36] *10^{-9}
L_{s1}	h	N [10.74, 0.18] *10^{-6}
L_{s2}	h	N [16.26, 0.27] *10^{-6}
x_0	m	U [0, 0.2]
y_0	m	U [-0.2, 0.2]

that there are no substantial disparities. Further observation of the EME at the heart reveals that the induced-E of the heart with an AVS is significantly higher than that of the heart without implants, and this leads to the position of the maximum induced-E in the human body shifting from the feet to the heart. This proves that metal implants have a significant impact on the distribution of electromagnetic fields in the human body, and lead to a maximum increase of induced-E in the human body by more than 1.76 times, increasing the risk of human EME safety.

B. Comparison of male and female human exposure considering uncertainty

In the practical application of the EV-WPT system, there are usually many uncertain factors, such as the offset parameters of the transmitting and receiving coils, resonance compensation circuit parameters, metal implant parameters, and position parameters between the human body and the EV. In this paper, the above parameters are used as input variables for quantifying the safety uncertainty of human EME, and different distribution types and parameters are set according to the daily use of the EV-WPT system. These variables are also inputs to the deep neural network, as shown in Table 2 . Among them, N is a normal distribution, corresponding parameters are mean and standard deviation, U is a uniform distribution, and corresponding parameters are lower and upper boundaries. Due to the consideration of the situation with an AVS in this paper, the maximum value of induced-E in the central organ of the human body is used as the output for quantifying the safety uncertainty of human EME. The probability density distribution curves of induced-E for both male and female genders are compared, and the results of 2000 Monte Carlo simulations are compared to verify the effectiveness of the proposed deep learning method, as shown in Fig. 13 .

The standard limit for human induced-E in ICNIRP 2010 is 11.5 V/m. Using this value as the judgment standard, the probability of male induced-E exceeding the standard limit is calculated to be 66.67%, while the probability of female induced-E exceeding the standard limit is 43.89%. This intuitively demonstrates the risk of human exposure to the electromagnetic environment of the EV-WPT system, and the probability of male EME is higher than that of female. According to the

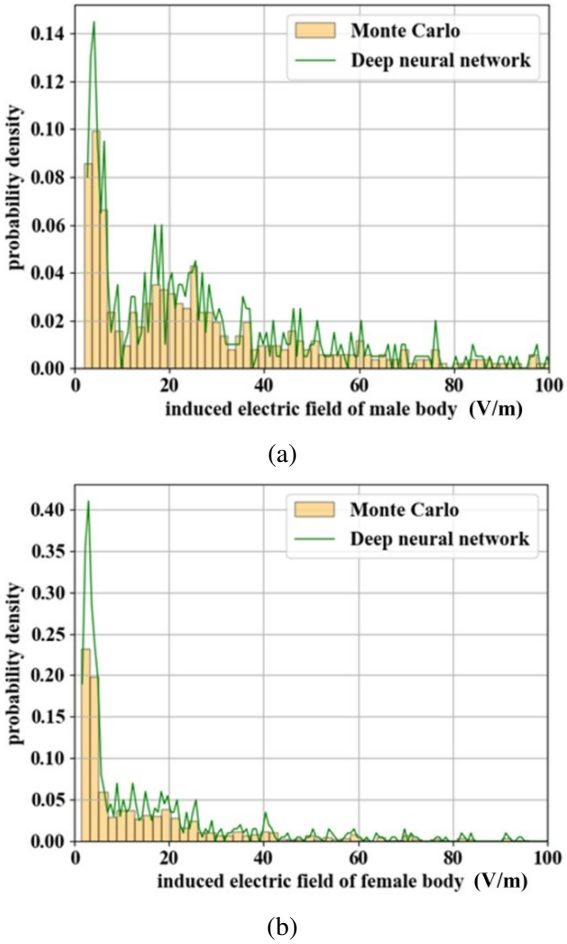

Fig. 13. (a) Probability density distribution of induced-E in male human EME and (b) probability density distribution of induced-E in female human EME.

analysis of EME in different genders under static conditions, the maximum value of induced-*E* in humans with AVS is usually located at the heart position, while the body thickness of female at the heart position is higher than that of male. Therefore, in the case of humans with AVS, the EME risk of female is lower than that of male due to the shielding effect of the female human body.

VI. CONCLUSION

The main purpose of this paper is to evaluate the safety issues of different genders of humans with AVS exposed to electromagnetic fields in the EV-WPT system. In the electromagnetic environment of the 11 kW transmission power EV-WPT system established in this paper, considering the uncertainty of the EV-WPT system, human EME position, and AVS parameters, the EME safety of different genders is evaluated for the scenario where the human body is located at the rear of the vehicle, which has a high risk of EME. The results indicate that, under static conditions, AVS can significantly alter the distribution of electromagnetic fields in the human body, leading to a maximum increase of induced-*E* in the human body by more than 1.76 times. Under the condition of considering uncertainty, due to the differences in human body between different genders, the risk probability of induced-*E* exceeding the standard limit in a male body is 66.67%, while the risk probability in a female body is 43.89%. In the following research, we will consider more human EME situations and, in order to protect the safety of human EME, we will conduct research on human electromagnetic safety protection devices.

ACKNOWLEDGMENT

This work is supported by the National Key Research and Development Program of China (2022YFE0123600). This paper is also supported by the Jilin Scientific and Technological Development Program under Grant 20240101117JC, Grant 20230201122GX, and Key Laboratory for Comprehensive Energy Saving of Cold Regions Architecture of Education, Jilin Jianzhu University under Grant JLJZHDKF202203.

REFERENCES

[1] P. Machura, V. De Santis, and Q. Li, "Driving range of electric vehicles charged by wireless power transfer," *IEEE Trans. Veh. Technol.*, vol. 69, no. 6, pp. 5968-5982, June 2020.

[2] W. Zhang and C. C. Mi, "Compensation topologies of high-power wireless power transfer systems," *IEEE Trans. Veh. Technol.*, vol. 65, no. 6, pp. 4768-4778, June 2016.

[3] H. Zhou, A. Zhu, Q. Deng, J. Chen, F. Yang, and W. Hu, "Protection strategy for wireless charging electrical vehicles," *IEEE Trans. Veh. Technol.*, vol. 69, no. 11, pp. 13510-13520, Nov. 2020.

[4] J. M. Miller, O. C. Onar, and M. Chinthavali, "Primary-side power flow control of wireless power transfer for electric vehicle charging," *IEEE Trans. Emerg. Sel. Topics Power Electron.*, vol. 3, no. 1, pp. 147-162, Mar. 2015.

[5] P. Moreno-Torres Concha, P. Velez, M. Lafoz, and J. R. Arribas, "Passenger exposure to magnetic fields due to the batteries of an electric vehicle," *IEEE Trans. Veh. Technol.*, vol. 65, no. 6, pp. 4564-4571, June 2016.

[6] International Commission on Non-Ionizing Radiation Protection, "Guidelines for limiting exposure to time-varying electric and magnetic fields (1 Hz to 100 kHz)," *Health Phys.*, vol. 99, pp. 818-836, 2010.

[7] International Commission on Non-Ionizing Radiation Protection, "Gaps in knowledge relevant to the 'Guidelines for limiting exposure to time-varying electric and magnetic fields (1 Hz-100 kHz)," *Health Phys.*, vol. 118, no. 5, pp. 533-542, 2020.

[8] "IEEE Standard for Safety Levels with Respect to Human Exposure to Electric, Magnetic, and Electromagnetic Fields, 0 Hz to 300 GHz," *IEEE Standard C95.1*, 2019.

[9] "Wireless Power Transfer for Light-Duty Plug-in/Electric Vehicles and Alignment Methodology," SAE Standard J2954_202010 [Online]. Available: https://www.sae.org/standards/content/j2954_202010/

[10] L. Perpétuo, A. S. Barros, J. Dalsuco, R. Nogueira-Ferreira, P. Resende-Gonçalves, I. Falcão-Pires, R. Ferreira, A. Leite-Moreira, F. Trindade, and R. Vitorino, "Coronary artery disease and aortic valve stenosis: A urine proteomics study," *Int. J. Mol. Sci.*, vol. 23, no. 21, pp. 13579, Nov. 2022.

[11] M. Kim, W. Lee, K. Kim, H. Lim, and Y. J. Kim, "A preclinical trial of periventricular pulmonary valve implantation: Pericardial versus aortic porcine valves mounted on self-expandable stent," *Artif. Organs.*, vol. 45, no. 5, pp. E89-E100, Oct. 2020.

[12] D. Poljak, M. Cvetković, O. Bottauscio, A. Hirata, I. Laakso, and E. Neufeld, "On the use of conformal models and methods in dosimetry for nonuniform field exposure," *IEEE Trans. Electromagn. Compat.*, vol. 60, no. 2, pp. 328-337, Apr. 2018.

[13] J. Xi, A. Christ, and N. Kuster, "Coverage factors for efficient demonstration of compliance of low-frequency magnetic near-field exposures with basic restrictions," *Phys. Med. Biol.*, vol. 68, no. 3, Feb. 2023.

[14] A. El-Shahat, J. Danjuma, A.Y. Abdelaziz, and S. H. E. Abdel Aleem, "Human exposure influence analysis for wireless electric vehicle battery charging," *Clean Technol.* vol. 4, no. 2, pp. 785-805, 2022.
[15] J. Chakarothai, K. Wake, T. Arima, S. Watanabe, and T. Uno, "Exposure evaluation of an actual wireless power transfer system for an electric vehicle with near-field measurement," *IEEE Trans. Microw. Theory Techn.*, vol. 66, no. 3, pp. 1543-1552, Mar. 2018.
[16] B. Choi, E. Kim, W. Shin, S. Park, and K. Kim. "Exposure assessment of a 20-kW wireless power transfer system for electric vehicles," *Int. J. Automot. Technol*., vol. 21, pp. 1349-1353, 2020.
[17] A. Christ, M. G. Douglas, J. M. Roman, E. B. Cooper, A. P. Sample, and B. H. Waters, "Evaluation of wireless resonant power transfer systems with human electromagnetic exposure limits," *IEEE Trans. Electromagn. Compat.*, vol. 55, no. 2, pp. 265-274, Apr. 2013.
[18] S. Park, "Evaluation of electromagnetic exposure during 85 kHz wireless power transfer for electric vehicles," *IEEE Trans. Magn.*, vol. 54, no. 1, pp. 1-8, Jan. 2018.
[19] Q. Wang, W. Li, J. Kang, and Y. Wang, "Electromagnetic safety evaluation and protection methods for a wireless charging system in an electric vehicle," *IEEE Trans. Electromagn. Compat.*, vol. 61, no. 6, pp. 1913-1925, Dec. 2019.
[20] I. A. Shah, Y. Cho, and H. Yoo, "Safety evaluation of medical implants in the human body for a wireless power transfer system in an electric vehicle," *IEEE Trans. Electromagn. Compat.*, vol. 63, no. 3, pp. 681-691, June 2021.
[21] I. A. Shah and H. Yoo, "Assessing human exposure with medical implants to electromagnetic fields from a wireless power transmission system in an electric vehicle," *IEEE Trans. Electromagn. Compat.*, vol. 62, no. 2, pp. 338-345, Apr. 2020.
[22] T. Wang, Q. Yu, B. Li, G. Lv, Y. Wu, and S. Guan, "Uncertainty quantification of human electromagnetic exposure from electric vehicle wireless power transfer system," *IEEE Trans. Intell. Transp. Syst.*, vol. 24, no. 8, pp. 8886-8896, Aug. 2023.
[23] T. Wang, B. Li, K. Zhao, Q. Yu, L. Xu, Y. Chi, and S. Guan, "Evaluation of electromagnetic exposure of the human with a coronary stent implant from an electric vehicle wireless power transfer device," *Electronics*, vol. 12, no. 20, p. 4231, 2023.
[24] M. Aenis, A. P. Stancampiano, A. K. Wakhloo, and B. B. Lieber, "Modeling of flow in a straight stented and nonstented side wall aneurysm model," *J. Biomech. Eng*., vol. 119, no. 2, pp. 206-212, May 1997.
[25] T. Ando and H. Takagi, "Percutaneous closure of paravalvular regurgitation after transcatheter aortic valve implantation: A systematic review," *Clin. Cardiol*., vol. 39, no. 10, pp. 608-614, 2016.
[26] A. Christ, M. Douglas, J. Nadakuduti, and N. Kuster, "Assessing human exposure to electromagnetic fields from wireless power transmission systems," *Proc. IEEE*, vol. 101, no. 6, pp. 1482-1493, June 2013.

Tianhong Tan received the B.S. degree in electrical engineering from Jilin University, Changchun, Jilin, China, in 2014. He is currently pursuing the Ph.D. degree in Information and Communication Engineering at Harbin Engineering University. His research interests include the electromagnetic compatibility, electromagnetic simulation and effectiveness evaluation

Tao Jiang received the Ph.D. degree from the Harbin Engineering University, Harbin, China, in 2002. Since 1994, he has been a Faculty Member of College of Information and Communication, Harbin Engineering University, where he is currently a Professor. He was a Postdoctoral Researcher with the Research Institute of Telecommunication, Harbin Institute of Technology, Harbin, China, from 2002 to 2003, and a Visiting Scholar with the Radar Signal Processing Laboratory, National University of Singapore, from 2003 to 2004. His current research interests include radio wave propagation, complex electromagnetic system evaluation, modeling, and simulation. IEEE Member 85027296.

Yangyun Wu received the B.S. degree in architectural electricity and intelligence from the College of Electrical and Informational Engineering, Jilin University of Architecture and Technology, Changchun, Jilin, China, in 2018, and the M.S. degree in electrical engineering from the College of Electrical and Computer Science, Jilin Jianzhu University, Changchun, in 2021. He is currently pursuing the Ph.D. degree in electrical engineering with the College

of Instrumentation and Electrical Engineering, Jilin University. His research interests include the uncertainty quantification and optimal design strategy of EV's wireless power transfer systems.

Yu Zhu received the M.S. degree and Ph.D. degree in measuring and testing technologies and instruments from Jilin University, Changchun, Jilin, China, in 2013 and 2021, respectively, where he is an associate professor with the College of Instrumentation and Electrical Engineering. His research interests include the analysis method in electromagnetic compatibility simulation and the uncertainty analysis methods in electromagnetic compatibility simulation.

Yaodan Chi received the B.S. degree in electronic information engineering from the Jilin University of Technology, Changchun, Jilin, China, in 1998, and the master's degree in testing and measuring technology and instruments and the Ph.D. degree in science and technology of instrument from Jilin University, Changchun, Jilin, China, in 2004 and 2018, respectively. She is currently the Vice Director of the Jilin Provincial Key Laboratory of Architectural Electricity and Comprehensive Energy Saving. Her research interests include the uncertainty analysis approaches in electromagnetic compatibility simulation and building equipment intelligent integration technology.